Bond-stretching force constants and vibrational frequencies in ternary zinc-blende alloys: A systematic comparison of (In,Ga)P, (In,Ga)As and Zn(Se,Te)

S. Eckner[1] [(a)(b)], A. Johannes[1] , M.Gnauck[1] , H. Kämmer[1] , T. Steinbach[1] , S. Schönherr[1] , R. Chernikov[2] [(c)], E. Welter[2] , M. C. Ridgway[3] , and C. S. Schnohr[1] [(b)]

[1] *Institut für Festkörperphysik, Friedrich-Schiller-Universität Jena, Max-Wien-Platz 1, 07743 Jena, Germany*
[2] *DESY Photon Science, Notkestrasse 85, 22607 Hamburg, Germany*
[3] *Department of Electronic Materials Engineering, Research School of Physics and Engineering, The Australian National University, Canberra ACT 0200, Australia*

*** Missing PACS ***

Abstract – We present element-specific effective bond-stretching force constants and Einstein frequencies of (In,Ga)P ternary alloys determined by temperature-dependent extended x-ray absorption fine structure spectroscopy. The bond-stretching force constants of both bond species show a nearly linear composition dependence between the values of GaP and InP. In contrast, the corresponding Einstein frequencies are different for the two bond species over the whole compositional range. Furthermore, we demonstrate that the composition dependence of bond-stretching force constants and Einstein frequencies for (In,Ga)P, (In,Ga)As, and Zn(Se,Te) is mostly caused by the associated bond length changes. Remaining deviations may be explained by coupling effects between different bond species within the alloy.

Introduction. – Compound semiconductors with zinc-blende structure offer a wide range of possibilities for application in electronic and opto-electronic devices, like high-performance transistors [1,2], nanolasers [3], and high-efficiency solar cells [4]. Random ternary and quaternary alloys of these materials are used to specifically tailor their properties, especially the lattice constant and the band gap energy [5].

While many properties of ternary alloys change continuously between those of the binary parent materials, the description and prediction of vibrational properties of random alloys is still challenging [6, 7]. In particular, the different types of disorder, namely in atomic masses, bond lengths and force constants, which form on the microscopic and mesoscopic scale, necessitate a detailed analysis of the interplay between local and macroscopic properties.

Two different measures commonly used to characterize the bond strengths of semiconductors are the elastic force constants calculated from the elastic moduli [8, 9], and the mode frequencies determined with Raman or infrared spectroscopy [6]. However, the two properties are very different in nature since elastic force constants describe macroscopic static properties averaged over the whole crystal whereas Raman mode frequencies cover the dynamics of single vibrational modes. A third measure are the effective force constants determined with temperature-dependent or pressure-dependent extended x-ray absorption fine structure (EXAFS) spectroscopy [10, 11]. Similar to the elastic force constants, they describe the bond strength between two atoms with a spring-like behaviour. However, bond force constants determined from elastic constants are accessible only for ordered compounds, while EXAFS facilitates the determination of *element-specific* bond-stretching force constants also in random alloys [7, 12]. Furthermore, elastic force constants describe the response to static stress and strain, whereas the force constants determined from temperature-dependent EXAFS are dynamic properties describing relative vibrations of neighbouring atoms. The corresponding Einstein frequencies therefore suggest comparability with Raman mode frequencies. However, Einstein frequencies can be thought

[(a)] Email: Stefanie.Eckner@physik.uni-leipzig.de
[(b)] current address: Felix-Bloch-Institut für Festkörperphysik, Universität Leipzig, Linnéstraße 5, 04103 Leipzig, Germany
[(c)] current address: Canadian Light Source, 44 Innovation Boulevard, Saskatoon, SK S7N 2V3, Canada

of as a weighted average over the whole phonon spectrum, therefore integrating all vibrational modes in contrast to the single mode frequencies of Raman spectroscopy [7].

Hence, temperature-dependent EXAFS measurements represent a powerful technique that is complementary to Raman spectroscopy and measurements of elasticity in characterizing the vibrational behaviour of compound semiconductors with the unique advantage of yielding element-specific information even in random alloys.

We used temperature-dependent EXAFS measurements to determine the element-specific effective bond-stretching force constants in random (In,Ga)P alloys as a function of composition and we discuss similarities and differences to the behaviour known from Raman spectroscopy and elastic constants. Furthermore, we compare the composition dependence of force constants and Einstein frequencies in (In,Ga)P to the one known for (In,Ga)As [7] and Zn(Se,Te) [12] to draw a comprehensive picture of the vibrational properties in ternary zinc-blende alloys.

Experimental. – GaAs bulk wafers with a miscut of 10 % relative to the (100) direction were covered with an AlAs layer approximately 50 nm thick [13]. Three (In,Ga)P thin films were then grown via metal organic chemical vapour deposition on these AlAs intermediate layers. The crystalline quality of the (In,Ga)P films was confirmed with Rutherford backscattering spectroscopy (RBS). The compositions were determined using RBS and energy dispersive x-ray analysis yielding In contents of 0.36 ± 0.03, 0.51 ± 0.02 and 0.71 ± 0.02.

The (In,Ga)P thin films were covered with Apiezon black wax and the AlAs was selectively etched with 10 % HF [13, 14], separating the ternary layer from the GaAs substrate. The wax was removed using trichloroethene and the sample material was mixed with BN and thoroughly ground for 15 min. The homogenized powder was then filled into sample holders and sealed with Kapton tape to form samples suitable for EXAFS measurements in transmission mode. The samples absorbed between 25 % and 85 % of the incoming x-ray intensity 50 eV above the Ga- and In-K-edge. Equivalent BN-diluted samples of the binary materials GaP and InP were prepared from commercial bulk wafers.

EXAFS measurements at the Ga-K- and In-K-edge (10367 eV and 27940 eV, respectively) were performed in transmission mode at Beamline C of DORIS III at DESY, Germany. Ten different temperatures ranging from 18 to 295 K were applied using a liquid-He flow-through cryostat ensuring temperature stability better than 1 K. For the ternary samples, up to three spectra were taken at selected temperatures to confirm the reproducibility of the measurements and to improve the reliability of the results. The spectra show edge steps between 0.2 and 0.7 at the Ga-edge and between 0.15 and 0.7 at the In-edge. For one sample, spectra of both absorption edges are shown in the supplemental information.

Data analysis. – Data analysis was done using the software package Larch [15] with theoretical phase shifts and scattering amplitudes calculated using Feff9. [16] The fitting model based on the zinc-blende structure contained the first twelve scattering paths (some of them split into a Ga- and an In-containing path) to avoid a distortion of the first shell results due to the higher shell contributions [17]. The first single scattering path and the split second single scattering paths were parameterized with one set of parameters each (interatomic distance, variance and asymmetry parameter). The remaining paths, consisting of all single and multiple scattering paths with a half path length up to the fourth nearest neighbour distance, were described with three additional parameters using geometrical considerations. While the interatomic distances were left free to vary for each temperature, the variances and asymmetry parameters were constrained by a correlated Einstein model using all terms to the first order [18] based on the interatomic potential

$$V(x) = \frac{k_0}{2}x^2 - k_3x^3 + k_4x^4,$$

where x denotes the deviation of the instantaneous first nearest neighbour distance from its value at the potential minimum. Ignoring the quartic force constant k_4, this means that only the harmonic term remains for the variance, while the asymmetry parameter is described by one term proportional to the cubic force constant k_3. All potential parameters were assumed as temperature independent.

To confirm this approach, the unconstrained variances of the Ga-P and In-P distance distributions obtained from individual fits of the spectra at each temperature are shown in Fig. 1 as a function of temperature. They rise with rising temperature due to increasing thermal vibrations. This temperature dependence is represented very well by the correlated Einstein model, which is determined by the bond-stretching force constant k_0 and a static contribution to the variance as free parameters.

The amplitude reduction factor S_0^2 and the threshold energy E_0 were varied freely per sample in simultaneous fits of all spectra of this sample measured at a given absorption edge (see supplemental material for details). The degeneracy of each scattering path was fixed to the value expected for the composition measured for the sample under consideration.

The analysis parameters and settings were varied systematically for each sample and absorption edge to estimate the overall uncertainties of the resulting bond-stretching force constants (see supplemental material for details). These tests included variation of the background subtraction parameters (edge energy and rbkg parameter in Larch), the window function for Fourier transformation (k_{min}, k_{max}, tapering parameter dk, and weighting exponent kw), the fitting range (r_{min}, r_{max}, and tapering parameter dr), and the model used in the fit (different assumptions for threshold energy and amplitude reduction

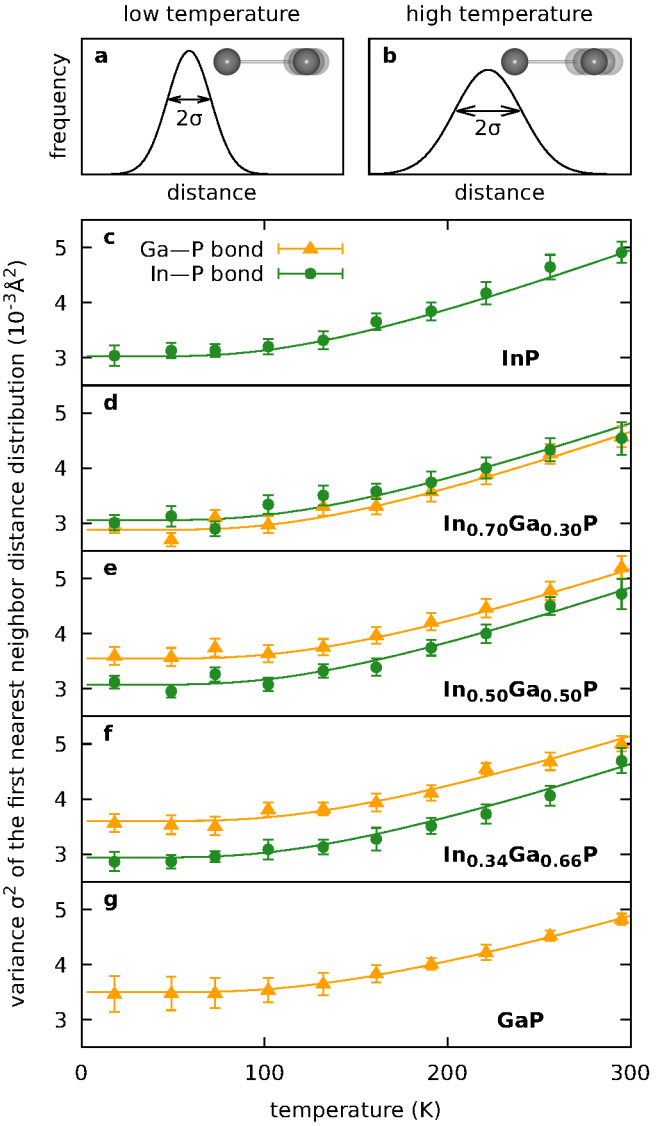

Figure 1: **a-b)** Schematic of the distance distribution stemming from static atomic displacements and thermal vibrations. As the amplitude of thermal vibrations increases with increasing temperature the width of the distribution, characterised by the standard deviation σ or the variance σ^2 (EXAFS Debye-Waller factor), increases, too. **c-g)** Temperature dependence of the variance of the first nearest neighbour distance distribution of the Ga-P bond (orange triangles) and In-P bond (green circles) determined with separate fits for each temperature. For all five samples measured, the data is represented very well by a correlated Einstein model (solid lines) with force constants and static contributions determined in simultaneous fits of all spectra of one sample at a given absorption edge.

factor and different parametrisations of second and third nearest neighbour scattering paths). The inclusion of anharmonic contributions to the variance and asymmetry parameter up to the third- and fourth-order perturbation [19] increased the bond-stretching force constants of the binary compounds by 5 to 10 % in good agreement with

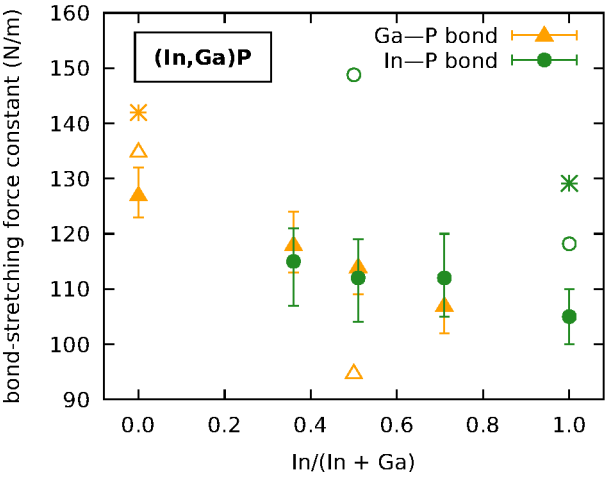

Figure 2: Effective bond-stretching force constants of the Ga-P bond (full orange triangles) and In-P bond (full green circles) in (In,Ga)P as a function of composition. The uncertainties were determined through systematic variation of the fitting procedure as described in the text. Theoretical predictions [20] (open symbols) and force constants determined from elastic constants of the binary materials [8] (stars) are depicted for comparison.

the effect of anharmonicity reported for CdTe [10]. The use of higher order anharmonic contributions in the description of the ternary alloys prevented the convergence of the fit. A meaningful comparison between all samples is therefore possible only for using the first order formulas for both the binary and ternary materials.

Results. – The resulting effective bond-stretching force constants are plotted in Fig. 2 and show a nearly linear composition dependence between the binary values. The bond-stretching force constant of 105 ± 5 N/m in InP is in good agreement with the value of 107 ± 4 N/m found in previous EXAFS studies [17, 21].

Different naming conventions for force constants are used in the literature. Most notably, EXAFS studies refer to $k_0 = k_{||}$ and $k_\perp$ as parallel effective force constant and perpendicular effective force constant, respectively [10], or bond-stretching and bond-bending force constants, respectively [21]. In valence-force-field models the bond-stretching and bond-bending force parameters, α and β, respectively, are used [8]. These are related to the force constant k_r, which operates as a bond-stretching force constant in the valence-force-field potential, as $k_r = 3\alpha + \frac{1}{2}\beta$ [8], where the contribution by the bending parameter β is often negligible. Raman studies can be discussed using a bond force constant including bond-stretching and bond-bending contributions [6] or separate force constants for stretching and bending [22].

The values 3α determined from measured elastic constants [8] for the binary materials GaP and InP are 10 to 20 % higher than the effective bond-stretching force constants determined by EXAFS (see Fig. 2). This behaviour

was observed before [5, 7, 21] and might be due to fundamental differences between the dynamic vibrational behaviour studied with EXAFS and the static response to stress and strain described by elastic constants [7]. The difference between the binary elastic force constants 3α of GaP and InP is comparable to the difference of the EXAFS effective bond-stretching force constants, despite the different absolute values.

Bond-stretching force parameters 3α predicted by a combination of first-principles density-functional theory and valence-force-field calculations [20] are plotted in Fig. 2 as open symbols. While the values reported for the binary materials are higher than the EXAFS effective bond-stretching force constants plotted in Fig. 2 as solid symbols, they reproduce well the EXAFS values determined using higher order anharmonic contributions in the fit. Again, the difference between the value for GaP and for InP is comparable to the difference of the two $k_{||}$ values.

In contrast to the experimental determination of 3α [8], the theoretical calculation offers the possibility to obtain bond-stretching force parameters for the individual bond species in the random alloy. As is visible in Fig. 2, the composition dependence is much more pronounced for these theoretically calculated values than for the EXAFS effective bond stretching force constants. Since the focus of that theoretical work was to reproduce formation energies rather than elastic properties, no explanation is given for the drastic change predicted for the force constants. Additionally, the force constants specified there relate to the values determined from elastic properties, hence they describe static behaviour. It is therefore not surprising that differences arise compared to the composition dependence of force constants determined with temperature-dependent EXAFS.

Discussion. –

Force constants and Einstein frequencies. A comparison of the first nearest neighbour effective bond-stretching force constants of (In,Ga)P, (In,Ga)As [7] and Zn(Se,Te) [12] is shown in Fig. 3. For Zn(Se,Te) the values were extracted from Fig. 4 in Pellicer-Porres *et al.* [12].The difference between the values of the binary compounds is approximately 20 N/m for (In,Ga)P and (In,Ga)As, while it amounts to only 10 N/m for Zn(Se,Te). In contrast to (In,Ga)P, a bond strength inversion is visible for (In,Ga)As and Zn(Se,Te), where the stiffer bond comparing the binary parent compounds is the softer bond comparing the bond species within one ternary sample. Interestingly, in both cases only one bond species, namely In-As in (In,Ga)As and Zn-Se in Zn(Se,Te), shows a significant deviation from the linear interpolation of the binary values (dashed black line in Fig. 3).

This impression changes when depicting the vibrational frequencies ν of the bonds calculated from the bond-stretching force constants k via $2\pi\nu = \sqrt{k/\mu}$, as done in Fig. 4. Since the conversion involves the reduced mass $\mu = m_A m_B/(m_A + m_B)$ of the bond A–B, the relation between the bond species can change when moving from bond-stretching force constants to Einstein frequencies. The two figures, Fig. 3 and Fig. 4, therefore contain the same information, but provide different perspectives on the vibrational behaviour.

While the two bond species in (In,Ga)P exhibit frequencies apart from each other over most of the compositional range, the frequencies of (In,Ga)As lie closer together and the ones of Zn(Se,Te) form one common curve. This suggests that coupling effects are more pronounced in Zn(Se,Te) and (In,Ga)As than in (In,Ga)P.

The amount to which mode coupling can occur in the alloy may be evaluated from the overlap of the phonon density of states of the binary parent materials. As a rough estimate the size of the frequency gap between the acoustic and optical modes of the stiffer binary compound, with the shorter bond length, can be used. If this gap is large, as the approximately 3 THz in GaP [23], the lower frequency optical modes of the longer bond species will lie within the gap. As a consequence mode coupling is inhibited, leading to two well separated Einstein frequencies in (In,Ga)P. If the gap is small or does not exist, as in GaAs [24, 25] and ZnSe [25], the optical modes of the longer bond species may couple to the acoustic modes of the shorter bond species. This may explain why the Einstein frequencies of (In,Ga)As and Zn(Se,Te) lie much closer together than for (In,Ga)P. With the additional simplification of relating the frequency gap between acoustic and optical modes at the Brillouin zone boundary to the masses of the vibrating atoms, the amount of mode coupling in the alloy would depend on the atom mass ratio of the shorter bond species, with a ratio near one enabling coupling.

Comparison with Raman measurements. Raman spectroscopy probes single modes at the Brillouin zone centre, while Einstein frequencies determined with EXAFS measurements depend on all vibrational modes over the whole Brillouin zone. Therefore, the vibrational properties measured by Raman spectroscopy differ substantially from those obtained by temperature dependent EXAFS measurements [7]. Nevertheless, it is informative to compare the results of both techniques. In Raman studies, (In,Ga)As shows two-mode behaviour, while (In,Ga)P and Zn(Se,Te) exhibit mixed-mode behaviour [6]. The Einstein frequencies of (In,Ga)As, in contrast, display a behaviour intermediate to that of (In,Ga)P and Zn(Se,Te) as shown in Fig. 4.

The percolation model, which was applied successfully to describe the Raman mode behaviour of ternary zinc-blende alloys [6, 26, 27], offers insight into the mechanisms underlying these vibrational properties. In the framework of the percolation model of random (A,B)C mixed crystals, the material is described as a composite of coexisting A-like and B-like regions [27], Due to slightly differing bond lengths within the two regions, they exhibit differing transversal optical (TO) mode frequencies leading to a

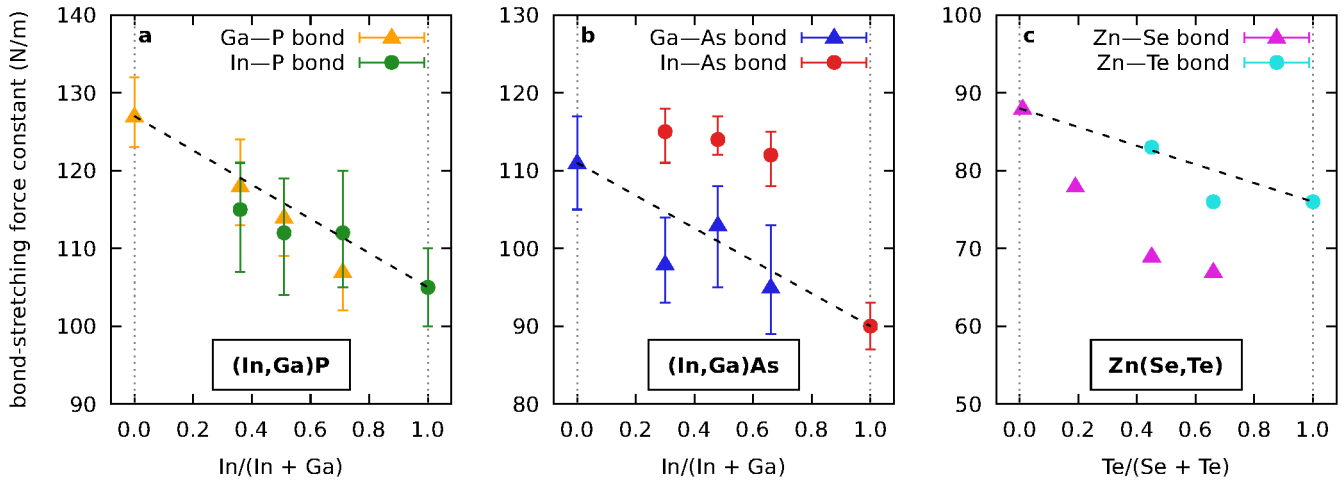

Figure 3: Element-specific effective bond-stretching force constants determined from temperature-dependent EXAFS measurements in three different ternary zinc-blende alloys. The uncertainties depicted for (In,Ga)P and (In,Ga)As [7] were determined through systematic variation of the fitting procedure. Uncertainties are expected to be larger for the Phosphides than for the Arsenides, since As is a stronger scatterer than P. Data for Zn(Se,Te) were extracted from Fig. 4 in Pellicer-Porres *et al.* [12], where no uncertainties are given. Black dashed lines visualize the straight connection between the binary values.

1-bond → 2-TO-mode percolation model. The frequency difference Δ of like TO modes in the dilute limit is one important input parameter needed to build up the percolation schemes of the materials studied [6].

When comparing these values, (In,Ga)P is set apart from (In,Ga)As and Zn(Se,Te) by the large splitting between like TO modes for one bond species, namely $\Delta_{\mathrm{InP:Ga}} > 20\,\mathrm{cm}^{-1}$, while all values are below $10\,\mathrm{cm}^{-1}$ in (In,Ga)As and Zn(Se,Te). [6] The extent of the TO-mode splitting is thought to increase with increasing bond length difference and increasing bond-stretching force constant due to anharmonic effects. [26,27] However, this does not explain the large difference between the splitting in (In,Ga)P and (In,Ga)As, indicating that additional effects are important. While it seems unlikely, that the differing TO-mode splitting causes differences in the composition dependence of Einstein frequencies, both may be affected by similar microscopic mechanisms.

In the framework of the percolation model, properties may change at the percolation threshold, dividing the composition range into a fractal-like regime (below the percolation threshold) and a normal regime (above the percolation threshold) [6]. Unfortunately, the fractal-like regime and the percolation threshold at 19 % minority bonds [6] are poorly covered by the Einstein frequency data. Nevertheless, hints for differences between the two regimes are visible for (In,Ga)As where the composition dependence of the In-As Einstein frequencies in the ternary alloys does not extrapolate to the binary value of InAs (see Fig. 4b). The same may be true for the Ga-As bonds in (In,Ga)As and the In-P bonds in (In,Ga)P, although the uncertainties preclude a final judgment in these cases. The other bonds, namely Ga-P in (In,Ga)P and Zn-Se and Zn-Te in Zn(Se,Te) show no sign of trend differences between binary and ternary values.

Bond length dependence. While the discussion up to now used the extended-mode picture, additional insight can be gained through the local-bond picture, where the focus is on a single bond with its underlying interatomic potential [7]. The change of this potential with changing interatomic distance can be described by a bond Grüneisen parameter [10, 28]. Pressure-dependent EXAFS measurements of CdTe using quasi-harmonic analysis yield a linear relation between the bond Grüneisen parameter and the bond length [28] . Assuming that this linear dependence is valid for compression as well as expansion of the bond, the change of the vibrational frequency of the Cd-Te bond can be calculated as a function of the bond length change. The resulting curve is depicted as solid black line in Fig. 5.

Bond length changes can, in principle, be induced by temperature changes, the application of hydrostatic pressure, or alloying. With respect to alloying, the shorter bond species in an alloy is slightly elongated while the longer bond species slightly contracts in comparison to the natural bond lengths exhibited in the binary compounds [5]. Therefore, the bond length ratios in Fig. 5 are larger than one for Ga-P, Ga-As, and Zn-Se, but smaller than one for In-P, In-As, and Zn-Te.

Strikingly, most of the Einstein frequencies of the ternary alloys lie on the black curve originally describing the pressure dependence of Einstein frequencies in binary CdTe, despite the different cause of the bond length change. The agreement is especially good for (In,Ga)P, where even the small difference in slope between the two bond species is reproduced. This indicates that the composition dependence of vibrational frequencies and force constants in (In,Ga)P is caused solely by the compression or expansion of the bonds. The agreement between

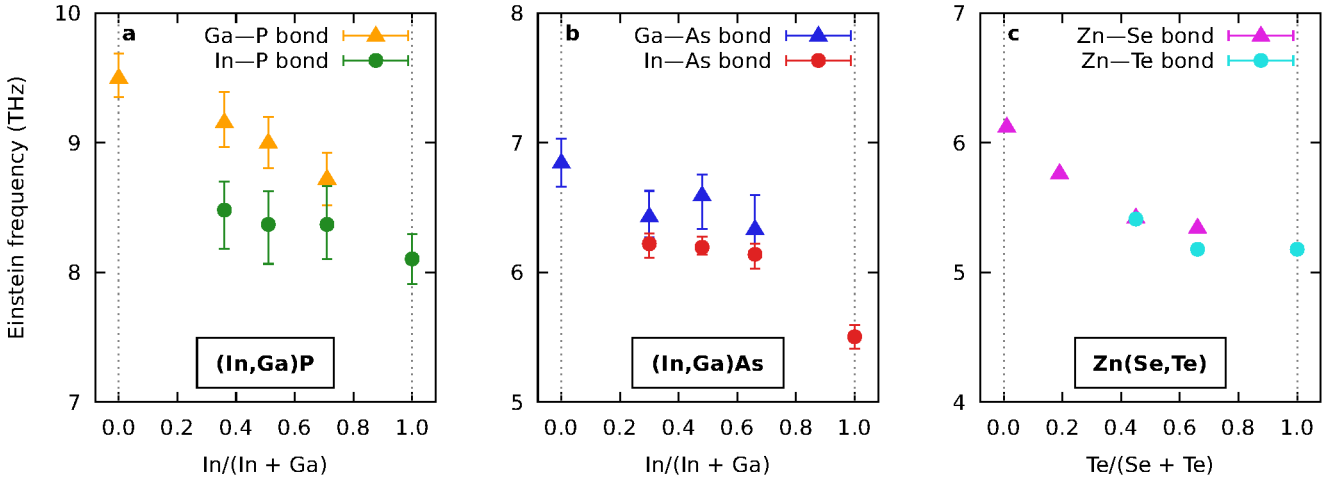

Figure 4: Einstein frequencies of first nearest neighbour bonds in three different ternary zinc-blende alloys. All values were calculated from the bond-stretching force constants shown in Fig. 3.

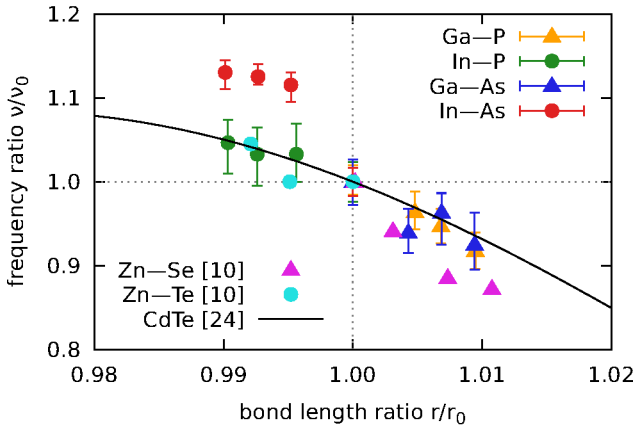

Figure 5: Change of Einstein frequency (ν) as a function of bond length (r) change, with ν_0 and r_0 denoting the corresponding values of the binary compounds.

Table 1: Reduced masses and Phillips ionicities of the different bond species [9]. The reduced mass was calculated from the atomic weights.

bond	reduced mass (amu)	ionicity
Ga-P	21.45	0.327
In-P	24.39	0.421
Ga-As	36.11	0.310
In-As	45.34	0.357
Zn-Se	35.77	0.630
Zn-Te	43.23	0.609

the different bond species hints at scaling laws existing for the parameters of the interatomic potentials in zinc-blende semiconductors.

Deviations from the common behaviour are visible for the In-As bond in (In,Ga)As and the Zn-Se bond in Zn(Se,Te). In both cases, the frequencies of the three ternary alloys exhibit a slope consistent with that of the CdTe curve. However, the values are offset because the difference between the binary compound at $\nu/\nu_0 = r/r_0 = 1$ and the closest ternary alloy is much larger than the corresponding change of the CdTe curve. This may indicate the importance of the percolation threshold previously discussed with the difference that here the effect is visible in the properties of the majority bond species.

The magnitude of the deviation is larger for the In-As bond than for the Zn-Se bond. Since coupling effects will not shift the frequency under consideration beyond the frequency of the second bond species, the observed deviation is probably related to the difference in Einstein frequencies of the respective binary parent compounds. The differences between the binary frequency are approximately 1.5 THz and 1.0 THz for (In,Ga)As and Zn(Se,Te), respectively (see Fig. 4). Therefore, the deviation from the pressure-induced CdTe curve would be expected to be larger for the In-As bond than for the Zn-Se bond, in agreement with the observed behaviour.

In the local bond picture, the composition dependence of bond-stretching force constants is caused by the alteration of the individual bond (bond length changes and charge redistributions) and by the modification of the surrounding matrix (exchange of atoms with different vibrational properties) [7]. Since four out of six bond species follow the pressure-induced changes in Fig. 5, the dependence on bond length changes seems well described in terms of the interatomic potential and bond Grüneisen parameter. The deviations visible for In-As and Zn-Se bonds should thus be attributed to charge redistributions or matrix effects.

If the deviations are caused by matrix effects, the decisive mechanisms occurring in the matrix upon exchange of atoms could be bond length changes, force constant

changes or mass changes. Since (In,Ga)P and (In,Ga)As exhibit similar differences in both bond lengths and force constants, these cannot explain the different behaviour of the two alloys. The differences of the reduced masses of the bond species, listed in Tab. 1, are small for (In,Ga)P and larger for (In,Ga)As and Zn(Se,Te). This could, in principle, cause differing vibrational properties. Yet, the deviations from the pressure-induced curve are visible for the heavier In-As bond in (In,Ga)As and for the lighter Zn-Se bond in Zn(Se,Te), which is not reconcilable with the simple explanation of an effect based on the reduced mass of the bonds in the surrounding matrix.

The vibrational properties could, however, also be related to the Phillips ionicities of the different bond species under consideration. (In,Ga)P features a difference in Phillips ionicities of 0.094, while the differences for (In,Ga)As and Zn(Se,Te) amount to only 0.047 and 0.021, respectively (see Tab. 1) [9]. Interestingly, the In-As bond and the Zn-Se bond both belong to the more ionic binary parent material of their respective alloy. This offers the possible explanation that the more ionic bond has a less defined force constant and therefore its vibrational frequency is changed more easily by an altered surrounding matrix.

Conclusion. – In conclusion, temperature-dependent EXAFS measurements reveal a significant composition dependence of the individual bond strengths in (In,Ga)P. The element-specific effective bond-stretching force constants vary continuously between the values of the binary parent materials, while the Einstein frequencies are different for the two bond species. These results differ from the known behaviour of (In,Ga)As and Zn(Se,Te), where an inversion is visible for the bond-stretching force constants and both bond species exhibit similar Einstein frequencies.

Plotting the Einstein frequency ratio as a function of the bond length ratio, the (In,Ga)P data is in excellent agreement with pressure-dependent EXAFS measurements of binary CdTe. Therefore, the composition dependence of bond-stretching force constants and Einstein frequencies in (In,Ga)P is well accounted for by considering only bond length changes. In contrast, mode coupling effects, which may depend on the atomic masses and bond ionicities involved, must be taken into account for (In,Ga)As and Zn(Se,Te).

Acknowledgements. – We acknowledge H. H. Tan for the growth of the (In,Ga)P thin films. We thank O. Pagès for fruitful discussions regarding the percolation model and the behavior of optical phonon frequencies in ternary zinc-blende alloys. Parts of this research were carried out at Beamline C of DORIS III at DESY, a member of the Helmholtz Association (HGF). The research leading to these results has received funding from the Friedrich-Schiller-Universität Jena under the ProChance Initiative (2.11.3-A1/2012-01).

References

[1] del Alamo J. A., *Nature*, **479** (2011) 317.
[2] Tomioka K., Yoshimura M. and Fukui T., *Nature*, **488** (2012) 189.
[3] Chen R., Tran T.-T. D., Wei Ng K., Son Ko W., Chuang L. C., Sedgwick F. G. and Chang-Hasnain C., *Nat. Photon.*, **5** (2011) 170.
[4] Dimroth F., Grave M., Beutel P., Fiedeler U., Karcher C. *et al.*, *Prog. Photovolt: Res. Appl.*, **22** (2014) 277.
[5] Schnohr C. S., *Appl. Phys. Rev.*, **2** (2015) 031304.
[6] Pagès O., Postnikov A. V., Kassem M., Chafi A., Nassour A. and Doyen S., *Phys. Rev. B*, **77** (2008) 125208.
[7] Eckner S., Ritter K., Schöppe P., Haubold E., Eckner E. *et al.*, *Phys. Rev. B*, **97** (2018) 195202.
[8] Martin R. M., *Phys. Rev. B*, **1** (1970) 4005.
[9] Adachi S., *Properties of Group IV, III-V and II-VI Semiconductors* (John Wiley & Sons) 2005.
[10] Fornasini P. and Grisenti R., *J. Synchr. Rad.*, **22** (2015) 1242.
[11] Hung N. V., *J. Phys. Soc. Jap.*, **83** (2014) 024802.
[12] Pellicer-Porres J., Polian A., Segura A., Muñoz-Sanjosé V., Di Cicco A. and Traverse A., *J. Appl. Phys.*, **96** (2004) 1491.
[13] Schnohr C. S., Araujo L. L., Kluth P., Sprouster D. J., Foran G. J. and Ridgway M. C., *Phys. Rev. B*, **78** (2008) 115201.
[14] Decoster S., Glover C. J., Johannessen B., Giulian R., Sprouster D. J. *et al.*, *J. Synchr. Rad.*, **20** (2013) 426.
[15] Newville M., *J. Phys.: Conf. Ser.*, **430** (2013) 012007.
[16] Rehr J. J., Kas J. J., Vila F. D., Prange M. P. and Jorissen K., *Phys. Chem. Chem. Phys.*, **12** (2010) 5503.
[17] Schnohr C. S., Araujo L. L. and Ridgway M. C., *J. Phys. Soc. Jpn.*, **83** (2014) 094602.
[18] Yokoyama T., *J. Synchr. Rad.*, **6** (1999) 323.
[19] Haug J., Chassé A., Schneider R., Kruth H. and Dubiel M., *Phys. Rev. B*, **77** (2008) 184115.
[20] Biswas K., Franceschetti A. and Lany S., *Phys. Rev. B*, **78** (2008) 085212.
[21] Schnohr C. S., Kluth P., Araujo L. L., Sprouster D. J., Byrne A. P., Foran G. J. and Ridgway M. C., *Phys. Rev. B*, **79** (2009) 195203.
[22] Vogelgesang R., Ramdas A. K., Rodriguez S., Grimsditch M. and Anthony T. R., *Phys. Rev. B*, **54** (1996) 3989.
[23] Borcherds P. H., Kunc K., Alfrey G. F. and Hall R. L., *J. Phys. C : Solid State Phys.*, **12** (1979) 4699.
[24] Strauch D. and Dorner B., *J. Phys.: Condens. Mat.*, **2** (1990) 1457.
[25] Rajput B. D. and Browne D. A., *Phys. Rev. B*, **53** (1996) 9052.
[26] Pagès O., Tite T., Kim K., Graf P. A., Maksimov O. and Tamargo M. C., *J. Phys.: Condens. Mat.*, **18** (2006) 577.
[27] Pagès O., Souhabi J., Postnikov A. V. and Chafi A., *Phys. Rev. B*, **80** (2009) 035204.
[28] Fornasini P., Grisenti R., Irifune T., Shinmei T., Mathon O., Pascarelli S. and Rosa A. D., *J. Phys.: Condens. Mat.*, **30** (2018) 245402.